Ordering and phase separation in multi-principal-element metallic alloys: Contribution from mean-field atomic-scale modelling and simulation

Rémy Besson

▶ **To cite this version:**

Rémy Besson. Ordering and phase separation in multi-principal-element metallic alloys: Contribution from mean-field atomic-scale modelling and simulation. Journal of Alloys and Compounds, 2022, Journal of Alloys and Compounds, 898, pp.162842. 10.1016/j.jallcom.2021.162842 . hal-03531765

HAL Id: hal-03531765
https://hal.univ-lille.fr/hal-03531765

Submitted on 7 Oct 2022

HAL is a multi-disciplinary open access archive for the deposit and dissemination of scientific research documents, whether they are published or not. The documents may come from teaching and research institutions in France or abroad, or from public or private research centers.

L'archive ouverte pluridisciplinaire **HAL**, est destinée au dépôt et à la diffusion de documents scientifiques de niveau recherche, publiés ou non, émanant des établissements d'enseignement et de recherche français ou étrangers, des laboratoires publics ou privés.

Journal of Alloys and Compounds

Ordering and phase separation in multi-principal-element metallic alloys: Contribution from mean-field atomic-scale modelling and simulation

--Manuscript Draft--

Manuscript Number:	JALCOM-D-21-13834R1
Article Type:	Full Length Article
Keywords:	Multi-principal-element alloys; phase diagrams; Pair interactions; Mean-field thermodynamics; ordering and phase separation
Corresponding Author:	Rémy Besson Unité Matériaux et Transformations Métallurgie Physique et Génie des Matériaux: Unite Materiaux et Transformations Metallurgie Physique et Genie des Materiaux Villeneuve d'Ascq, FRANCE
First Author:	Rémy Besson
Order of Authors:	Rémy Besson
Abstract:	Multi-principal-element alloys (MPEAs) are a wide class of materials currently at the center of numerous investigations. Key-issues with MPEAs are related with controlling the onset of (i) long-range order and (ii) phase separation, both processes being in general detrimental to the properties. While trends (i) and (ii) are strongly dependent on the precise proportions of metallic elements around the reference equiatomic MPEA, the tremendously large composition space makes it a tricky task to heuristically identify optimized MPEAs. In practice, this often leads to undesired second-phase ordered particles. This deficiency emphasizes the relevance of modelling and simulation tools designed to facilitate the exploration of MPEA composition spaces. In this atomic-scale work, we propose a “composition-constrained” point mean-field formalism resting on alloy pair energetics, to investigate trends (i) and (ii). This formalism is currently applicable to a wide panel of such systems built from ~ 30 chemical elements. Its application to several MPEAs along the AlCoCrFeNi → AlCrFeMnNi → AlCrFeMnMo sequence evidences striking differences between these systems, and demonstrates its efficiency to get at-a-glance information about (i) and (ii) features for various MPEAs. The flexibility of the proposed simulation approach makes it easily employable in conjunction with experiments on well-equilibrated MPEA samples, for thermodynamic characterizations of MPEAs.
Order of Authors:	Rémy Besson

Powered by Editorial Manager® and ProduXion Manager® from Aries Systems Corporation

Revised Manuscript Click here to view linked References

Ordering and phase separation in multi-principal-element metallic alloys: Contribution from mean-field atomic-scale modelling and simulation

Rémy Besson
Univ. Lille, CNRS, INRAE, Centrale Lille, UMR 8207 - UMET - Unité Matériaux et Transformations, F-59000 Lille, France

ABSTRACT

Multi-principal-element alloys (MPEAs) are a wide class of materials currently at the center of numerous investigations. Key-issues with MPEAs are related with controlling the onset of (i) long-range order and (ii) phase separation, both processes being in general detrimental to the properties. While trends (i) and (ii) are strongly dependent on the precise proportions of metallic elements around the reference equiatomic MPEA, the tremendously large composition space makes it a tricky task to heuristically identify optimized MPEAs. In practice, this often leads to undesired second-phase ordered particles. This deficiency emphasizes the relevance of modelling and simulation tools designed to facilitate the exploration of MPEA composition spaces. In this atomic-scale work, we propose a "composition-constrained" point mean-field formalism resting on alloy pair energetics, to investigate trends (i) and (ii). This formalism is currently applicable to a wide panel of such systems built from ~ 30 chemical elements. Its application to several MPEAs along the AlCoCrFeNi → AlCrFeMnNi → AlCrFeMnMo sequence evidences striking differences between these systems, and demonstrates its efficiency to get at-a-glance information about (i) and (ii) features for various MPEAs. The flexibility of the proposed simulation approach makes it easily employable in conjunction with experiments on well-equilibrated MPEA samples, for thermodynamic characterizations of MPEAs.

INTRODUCTION

The growing interest for metallic multi-principal-element alloys (MPEAs), especially in the field of well-known "chemically complex alloys" (CCAs) or "high-entropy alloys" (HEAs), provides a strong motivation for a better understanding of their intricate physical properties [1]. Among the current topics of interest on MPEAs which strikingly illustrate this intricacy, it is worth mentioning recent investigations showing the good combination of mechanical and magnetic properties achievable in ultrafine-grained $FeCoNiCu_{0.2}Si_{0.2}$ alloys [2], the complex non-linear deformation behavior (Portevin-Le Chatelier effect) of Al-Mg-Cu-Zn medium-entropy Al-based alloys [3] or the high wear resistance of the CoCrFeMnNi Cantor alloy attributed to subsurface phase precipitation [4]. At the crossing of these various properties, thermodynamics plays a prominent role (see e.g. chapter 8 of Ref. [5]), since MPEAs are, at least partly, stabilized by high configuration entropy. The advantages of MPEAs are usually attributed to their nature of chemically intricate concentrated solid solutions (five or more metallic elements, often in roughly equal proportions), in which atomic disorder is expected to lead to significant beneficial effects, such as structural hardening by dislocation pinning, grain boundary strengthening… Therefore, it is an admitted fact that preserving these advantages, associated to the presence of a single-phase disordered solid solution, implies to avoid uncontrolled processes of long-range or strong short-range ordering as well as formation of unexpected other phases, in particular during the elaboration processes.

In this context, while practical elaboration of MPEAs therefore requires to take much care of obtaining single-phase cubic solid solutions (possibly further strengthened by dispersions of particles of long-range ordered compounds, but always in a well-controlled manner), recent experiments on body-centered cubic (bcc) AlCrFeMnMo [6] have confirmed the recurrence of simultaneous formation of undesired phases, such as carbides, with complex crystallography and chemistry including various degrees of order. Since these additional phases result from the various thermomechanical treatments included in the elaboration processes, their degree of (meta)stability is thus frequently unknown, which makes it difficult to ensure that the elaborated MPEAs will retain their single-phase solid solution structures and associated good properties in further applications. Central to handle this issue is the knowledge of the metallic chemical potentials in the MPEA solid solution, since these quantities directly determine the formation of additional phases, as well as the propensity of these phases to accept metallic elements coming from the surrounding MPEA. Considering the case of undesired carbides in AlCrFeMnMo, these questions have made the subject of recent investigations relying on atomic-scale models and simulations [7,8].

As a second issue more closely related to the present work, even ignoring these additional, frequently ordered, non-cubic complex phases, two major phenomena of high interest for MPEAs are still worth investigating, namely the occurrence, within the primary solid solution, of cubic-based various kinds of (i) long- or short-range orderings and (ii) phase separations, both features being strongly dependent on alloy composition and temperature, driving the MPEA away from the ideal single-phase solid solution structure, and thus being detrimental to its properties. For instance, the recent experimental investigations on AlCrFeMnMo [6] cited previously have also pointed out, as a function of the elaboration process, the possibility of simultaneous formation and spatial coexistence of two distinct disordered solid

solutions with different compositions, a feature not observed in other MPEAs (e.g. AlCoCrFeNi [9]) and thus apparently intriguingly alloy-dependent. However, no interpretation could be proposed for this specific behaviour of AlCrFeMnMo, especially as concerns the level of metastability of either solid solution observed. More generally, it would be useful to identify arguments allowing to interpret the sequence of events that may occur when cooling from high-temperature a single-phase MPEA solid solution, in order to help answer such questions as: at cooling, does long-range ordering occur prior to or later than phase separation? to which extent is such trend alloy-dependent? is it possible to identify physical factors governing these features for a given MPEA?

Therefore, when carrying out the elaboration and design of a new MPEA, it would be of great interest the have a deep knowledge of its equilibrium state, either full or cubic-restricted, but the latter is usually very difficult to determine by dedicated experiments such as annealing heat treatments. While this issue – determining the equilibrium state of an MPEA – could also in principle be efficiently tackled using phenomenological thermodynamic modellings and simulations, for instance via the well-known "CALculation of PHAse Diagrams" approach, a critical point in such approach comes from the fact that the databases currently proposed for MPEAs remain often "sparse" (from the point of view of the low density – in composition space – of the input data used to build them), which still casts some doubt on the validity of the predictions drawn from these databases. This leaves some room for lower-scale approaches, such as the one described in the present work.

Whatever the route, either phenomenological or atomic-scale, chosen for simulation studies of MPEA thermodynamics, a mostly desirable achievement would consist in being able to scan the aforementioned properties (i) and (ii) through wide composition domains, a task of high interest because it would make it possible to get a quick picture of a model MPEA with respect to these basic important properties, thus allowing easy comparison with reference experiments, and even model refinements through inverse fitting methods.

To investigate properties (i) and (ii), atomic-scale models for MPEA energetics based on relatively simple (restricted to short-range pairs) cluster expansions [10] provide a convenient framework, since they constitute a sound, relatively handsome and versatile basis to perform thermodynamic investigations of phase stability, thus easily comparable to experiments. Such models have already proved to be useful in various contexts including fairly complex steel-like alloys [11], which suggests that their extension to MPEAs could be relevant. Even restricted to pair interactions, it is not a trivial task to achieve a robust cluster expansion energy model for an alloy, via fitting procedures commonly employed to determine numerically the pair energy coefficients, and this difficulty, already significant and well documented in various binary and ternary systems, is enhanced critically when chemical complexity grows further, as is the case in five-element equiatomic MPEAs (a panel of ten such pair coefficients being required for each neighbour shell in a quinary system). In this intricate context, it is particularly appealing to consider the specific first-nearest neighbour (1NN) pair MPEA energetics proposed in a previous work [12] based on high-throughput ab initio calculations.

The relevance of this approach is further emphasized by the fact that the ab initio-based 1NN pair energetics proposed in this earlier work [12] covers a relatively large panel (~ 30) of chemical elements, thus a priori allowing theoretical investigations of a very high number of MPEA solid solutions, for which the aforementioned properties (i) and (ii) can be determined and compared. This may offer a valuable basis for the identification of general trends among an extended MPEA family.

Within this simplified 1NN pair scheme for alloy energetics, performing atomic-scale thermodynamic calculations on MPEAs still remains challenging, due to the rather high dimensionality of the composition space, which makes its exploration exceedingly cumbersome. While the main focus should a priori be given to the equiatomic alloy, departures from this reference case cannot be discarded in general, as illustrated e.g. in a recent experimental work on AlCrFeMnMo [6]: in this case, together with the equiatomic one, an alternative Fe-enriched Mo-depleted-composition was investigated. However, the selection of this second alloy was performed on rather heuristic grounds (resorting to frequently used empirical criteria for HEA selection, e.g. electronegativity or atomic volume), or even more practically, in order to reduce the alloy cost (high cost of Mo), a procedure which lacks physically justified information on the consequences of this empirical selection as regards alloy stability from thermodynamics. In this respect, the above frame for atomic-scale simulations may be useful to compare more rigorously candidate alloys, since it provides a quick route to investigate the expected effect on properties (i) and (ii) of elaboration choices such as Fe enrichment and Mo depletion.

To bring information on these issues, a previous work [13] was carried out by Monte-Carlo (MC) simulations using the above mentioned 1NN pair energetics. While this previous MC simulation work was primarily concerned with the interpretation of the experimental behaviour of AlCrFeMnMo, the approach was made more comprehensive and illustrative by considering three bcc MPEA systems, in order to monitor the effect of the AlCoCrFeNi → AlCrFeMnNi → AlCrFeMnMo sequence for alloy selection (corresponding to substitution of Co with Mn, followed by substitution of Ni with Mo). For each of these alloys, the predicted phase transformations at cooling were investigated and compared, showing significant similarities as well as discrepancies among these systems, as regards properties (i) and (ii). Most remarkably, following the phase evolution at cooling from the high-temperature ideal disordered (A2) solid solution, these simulations suggested that the emergence of B2-type long-range order should

occur in the single-phase domain, i.e. prior to any phase separation, for all alloys investigated. In contrast with this common predicted trend, the subsequent phase separation processes, occurring at lower temperatures, were found to be much more alloy-dependent: an ordered/disordered A2 + B2 morphology was found for the first two MPEAs, whereas a purely ordered B2' + B2'' mixture was predicted for AlCrFeMnMo. In the latter case, these simulation results were clearly at odds with the experiments recalled above [6], which suggested a purely disordered A2' + A2'' two-phase mixture. Another remarkable feature revealed by these simulations was the possibility of low-temperature emergence of a disordered A2 phase from the B2 single-phase state, a behaviour predicted for AlCoCrFeNi and AlCrFeMnNi. While this previous MC simulation study of AlCrFeMnMo surprisingly revealed that this MPEA should consist of two B2-type ordered phases at ambient temperature, instead of the couple of A2 solid solutions observed in practice, it also provided some hints that this discrepancy could be attributed to some deficiencies in the panel 1NN pair interactions, in particular those involving Mo, hence suggesting that the ab initio-based energetics proposed [12] might be improvable from this point of view (e.g. by including selectively 2NN interactions for Mo…). Alternatively, it may also indicate that the AlCrFeMnMo MPEA samples produced experimentally were significantly far from equilibrium and contained at least one metastable A2 phase. On the whole, checking such hypotheses is difficult, since it requires preparing highly equilibrated MPEA samples, whereas such samples are usually not the target of practical elaboration processes.

As a remarkable advantage over the simpler mean-field approaches forming the topic of the present work, it should be noted here that MC simulations are thermodynamically exact, i.e. they provide the exact thermodynamic behaviour of an MPEA system for the selected model alloy energetics. Moreover, while our work is limited to pair energy models, it is worth recalling that MC simulations can be used in conjunction with much more elaborate alloy energetics, including complex clusters of sites, and such possibilities have been used in recent works on MPEAs [14,15]. These are important points to keep in mind, our purpose being to assess properties (i) and (ii), either qualitatively or more accurately, including critical temperatures of phase transitions. However, such MC simulations could exclusively be carried out for a small panel of candidate MPEAs with selected compositions (i.e. simulations in the canonical statistical ensemble), and thus cannot be employed during the early stages of MPEA selection. Due to their high computational cost, they nowadays remain hardly applicable to explore in an exhaustive way MPEA composition spaces, a deficiency which emphasizes the relevance of complementary atomic-scale tools offering a better ability to comprehensive exploration of extended composition domains. To this purpose, semi-analytical mean-field approaches may be valuable, above all the cluster variation method (CVM) in the tetrahedron approximation, which seems to be particularly suitable to the context of MPEAs, since the latter often have cubic (bcc or fcc) structures. However, extending CVM to scan MPEA composition spaces is not as straightforward as expected, since this approach is usually formulated in a (semi-)grand canonical way, whereas it is desirable to handle composition constraints. In this respect, leaving CVM for further works, a valuable step for MPEA modelling probably consists in investigating these issues in a simpler manner, namely through a point mean-field (PMF) formalism, in close connection with previous investigations [11], which constitutes the topic of the present work. It is instructive to investigate the PMF weaknesses and merits for predicting properties of MPEAs, according several levels of analysis of increasing accuracies, namely: the general trends (i) and (ii), but also the quantitative estimations of critical (long-range ordering and phase separation) temperatures, the phases compositions, and the characterization of long-range ordering via sublattice occupancies by the various chemical species.

In the present work, we thus describe the application of composition-constrained PMF to quinary MPEAs. We make use of the 1NN pair energetics available in the literature, while the PMF approach is also suited to include 2NN pairs. We focus on bcc alloys, being primarily concerned with the ill-known AlCrFeMnMo system, but we also include in our analysis the more widely documented AlCoCrFeNi system. To investigate the strengths and weaknesses of PMF in the context of MPEAs, we also make appropriate comparisons with a previous work [13] concerned with the same alloys using MC simulations, taking the latter as a thermodynamically exact, reference case.

METHODS

As described in the introduction, the alloy energetics is supposed pairwise, restricted to first-nearest-neighbour (1NN) range, and taken from the ab initio-built elemental database provided in a previous work [12]. Although the five chemical elements play symmetrical roles, the pair cluster energy model on which the PMF formalism is built involves only pair coefficients J_{qN}^{ij} between elements other than i_0 = A (this choice of A as "background element" being immaterial). A conversion from the raw pairwise enthalpy parameters H^{ij} (for $i \neq j$ including A) taken from Ref. [12] towards the coefficients J_{1N}^{ij} (including i = j but discarding A) is thus required:

- $J_{1N}^{ii} = -\frac{2}{z_{1N}} H^{ii_0}$ for i_0 the chosen « background » element (Fe in this work) and $i \neq i_0$,
- $J_{1N}^{ij} = \frac{1}{z_{1N}} \left[H^{ij} - H^{ii_0} - H^{ji_0} \right]$ for $(i;j) \neq i_0$,

$z_{1N} = 8$ being the coordination number of the first-nearest-neighbour shell in the bcc structure. It can be noted that the ratios H^{ij}/z_{1N} are the so-called « interchange » energy parameters conveniently appearing in the alloy formation energy from the pure elements with same bcc structure. We make the choice A = Fe throughout in the present PMF calculations. While it is of course not possible, at this stage, to infer the overall effect of these energy parameters on MPEA thermodynamics, it can nevertheless be noticed that, among the various binary systems considered in Table 1, only two of them, i.e. Co-Cr and Cr-Mo, have positive H^{ij} parameters, respectively with weak (5 meV) and more significant (42 meV) values. The correspondingly negative J_{1N}^{ij} coefficients can then be related [11] to the well-known diagram of ground-states for binary systems with 1NN and 2NN pair interactions. This diagram allows to know which, among the possible (A2, B2, $D0_3$, B32) kinds of order, are to be expected at low temperature as function of the signs of J_{1N}^{ij} and J_{2N}^{ij}. The present case $J_{2N}^{ij} = 0$ yields a much simplified picture for the possible ground-states, namely either A2 or (A2,B2) for J_{1N}^{ij} negative or positive respectively. The positive H^{ij} parameters assumed for Co-Cr and Cr-Mo should thus promote the disordered A2 phase (interesting for HEAs), rather than B2-type order, in both binary systems, but these remarks are hardly transposable to quinary cases, for which such trends towards A2 may easily be thwarted by other interactions with opposite signs.

	Al	Co	Cr	Fe	Mn	Mo	Ni
Al	92	-25 (-629)	30 (-138)	x (-369)	10 (-278)	86 (-168)	-26 (-677)
Co	-25 (-629)	15	9 (5)	x (-60)	x	X	17 (-21)
Cr	30 (-138)	9 (5)	2	x (-8)	-14 (-110)	67 (42)	9 (-30)
Fe	x (-369)	x (-60)	x (-8)	x	x (9)	x (-484)	x (-97)
Mn	10 (-278)	x	-14 (-110)	x (9)	-2	42 (-136)	-3 (-115)
Mo	86 (-168)	x	67 (42)	x (-484)	42 (-136)	121	X
Ni	-26 (-677)	17 (-21)	9 (-30)	x (-97)	-3 (-115)	X	24

Table 1: First-nearest-neighbour pair energy coefficients J_{1N}^{ij} (meV) useful for PMF calculations for the various MPEA systems considered, as deduced from the H^{ij} pairwise enthalpy parameters (meV) provided in Ref. [12] and recalled between parentheses. The conversion from H^{ij} to J_{1N}^{ij} is described in the text. Empty entries marked "x" correspond to pairs of elements either absent from the MPEAs studied or not required in the PMF modelling (i.e. pairs involving Fe, since the latter was chosen as "background element").

We now present briefly the PMF formalism for an A-B-C-D-E quinary substitutional bcc alloy with two composition constraints on elements D and E. This "constrained PMF" approach, which allows convenient 2D display of the quinary phase diagram via isothermal pseudo-ternary sections, should be easily generalizable to higher-order (senary...) systems, by straightforward increase of the number of composition constraints. A similar PMF methodology was described in a previous paper [11] for quaternary steel-like alloys containing three substitutional metallic elements and interstitial carbon, in which case a single constraint (constant amount of C) was handled. The extension of this approach to quinary substitutional MPEAs, including two composition constraints and leaving aside interstitial sublattices, can be carried out easily as follows.

For substitutional bcc alloys, the well-known decomposition into four sublattices $S \in \{\alpha, \beta, \gamma, \delta\}$ (the α and β sublattices being chosen on the same cube, idem for γ and δ) is relevant, hence for a quinary system A-B-C-D-E, a 16-element set of PMF variables $\{c_S^B, c_S^C, c_S^D, c_S^E\}$. The PMF formalism is conveniently formulated in grand canonical form, adding to the Hamiltonian a chemical potential term proportional to the amounts of chemical species. Minimizing the PMF free energy functional with respect to the PMF variables $\{c_S^B, c_S^C, c_S^D, c_S^E\}$ then yields, for B occupancy on sublattice S_0:

$$\sum_q \sum_S z_{S(S_0)}^{qN} \left[J_{qN}^{BB} c_S^B + J_{qN}^{BC} c_S^C + J_{qN}^{BD} c_S^D + J_{qN}^{BE} c_S^E \right] + J_1^B - \mu^B + \mu^A + kT \ln \frac{c_{S_0}^B}{1 - c_{S_0}^B - c_{S_0}^C - c_{S_0}^D - c_{S_0}^E} = 0$$

also written as:

$$G_{S_0}^B\left(\{c_S^B, c_S^C, c_S^D, c_S^E\}\right) + kT \ln \frac{c_{S_0}^B}{1 - c_{S_0}^B - c_{S_0}^C - c_{S_0}^D - c_{S_0}^E} = 0$$

and which can be inverted into:

$$c_{S_0}^B = \frac{X_{S_0}^B}{1 + X_{S_0}^B + X_{S_0}^C + X_{S_0}^D + X_{S_0}^E}$$

with $X_{S_0}^B\left(\{c_S^B, c_S^C, c_S^D, c_S^E\}\right) \triangleq e^{-G_{S_0}^B/kT}$. Similar expressions hold for $c_{S_0}^C$, $c_{S_0}^D$ and $c_{S_0}^E$ (with $S_0 \in \{\alpha, \beta, \gamma, \delta\}$), providing a set of coupled non-linear equations.

The constraint on the D atomic fraction x_D is:

$$x_D = \frac{1}{4}\sum_S c_S^D$$

and a similar expression holds for the constraint on x_E. The chemical potentials μ^D and μ^E then become additional variables determined implicitly at each PMF iteration. In practice, using this "constrained PMF" requires to perform a double scan in B and C chemical potentials (the quantities scanned being $\delta\mu^B = \mu^B - \mu^A$ and $\delta\mu^C = \mu^C - \mu^A$), while the D and E chemical potentials $\delta\mu^D$ and $\delta\mu^E$ fulfilling the constraints on x_D and x_E are determined for each ($\delta\mu^B$; $\delta\mu^C$).

Before turning to PMF results for MPEA thermodynamics, it is worth mentioning briefly technical issues related to the convergence of the PMF algorithm, since the latter was sometimes found to be trapped and display a non-convergent oscillating behaviour (Figure 1). This issue, which occurs at low temperatures only, may be critical in practice, because it may lead to spurious PS domains (as illustrated in the next section), through the erroneous labelling as PS of points absent from the phase diagram due to a lack of convergence of the PMF algorithm for particular ranges of chemical potentials. Noticeably, at a given iteration of the PMF algorithm showing such oscillations, i.e. for the current values of the PMF variables (sublattice occupancies), this oscillating behaviour is not related to the internal solving, which is in most cases quickly convergent, of constraints for constant x_D and x_E (namely the internal solving for D and E chemical potentials), but mainly to the PMF fixed point algorithm itself. Fortunately, this PMF oscillating behaviour could be eliminated, at least partially, by modifying the choice of initial values for the PMF variables, in particular by starting from the converged values obtained at a slightly higher temperature for the same B and C chemical potentials.

Nevertheless, it should be noted that this oscillating PMF behaviour may not be due solely to inappropriate choices of initial values, since it may also a priori have a more physical origin, related to occurrence of PS domains: in the latter situation, the required composition constraints on x_D and x_E may simply not be achievable for some B and C chemical potentials. This is illustrated on Figure 2, for the simpler case of a ternary system with a single constraint: whereas PMF convergence is ensured in the "usual" case (depicted on Figure 2a) for which the PMF solution (isopotential-constraint crossing point) exists, the algorithm may become oscillating (between the couple of points shown as red circles on Figure 2b) if the crossing point falls within a PS domain.

However, at odds with the typical case illustrated on Figure 2b, we could not detect, throughout the quinary MPEAs considered in this work, situations showing explicit connection between oscillating PMF and PS domains, and we thus could not determine to which extent this behaviour is related to truly unachievable constraints. In addition, PS domains are also related to the limiting cases $\delta\mu^B = \delta\mu^B{}_1$ and $\delta\mu^B = \delta\mu^B{}_2$ (Figure 2c) which are therefore interesting to consider, all the more as they can be related to behaviours obtained in practice for quinary systems (Figure 2d). It should also be remarked that, while for the ternary system sketched on Figure 2c these limiting cases should in general correspond to discontinuities of both $\delta\mu^B$ ($\delta\mu^B{}_1 \neq \delta\mu^B{}_2$ on Figure 2c) and $\delta\mu^C$ across the PS domain, the quinary systems studied in this work displayed somewhat different behaviours (as depicted on Figure 2d), such as continuous $\delta\mu^B$ and discontinuous ($\delta\mu^D$;$\delta\mu^E$). These more intricate features are probably related to the fact that for higher-order systems, isopotentials are non-planar paths in composition space. On the whole, and fortunately, these rather subtle technical issues related to PMF convergence and PS domains were not found critical for our purpose, as demonstrated below, in so far as they did not prevent us from using PMF to investigate the LRO and PS trends of MPEAs.

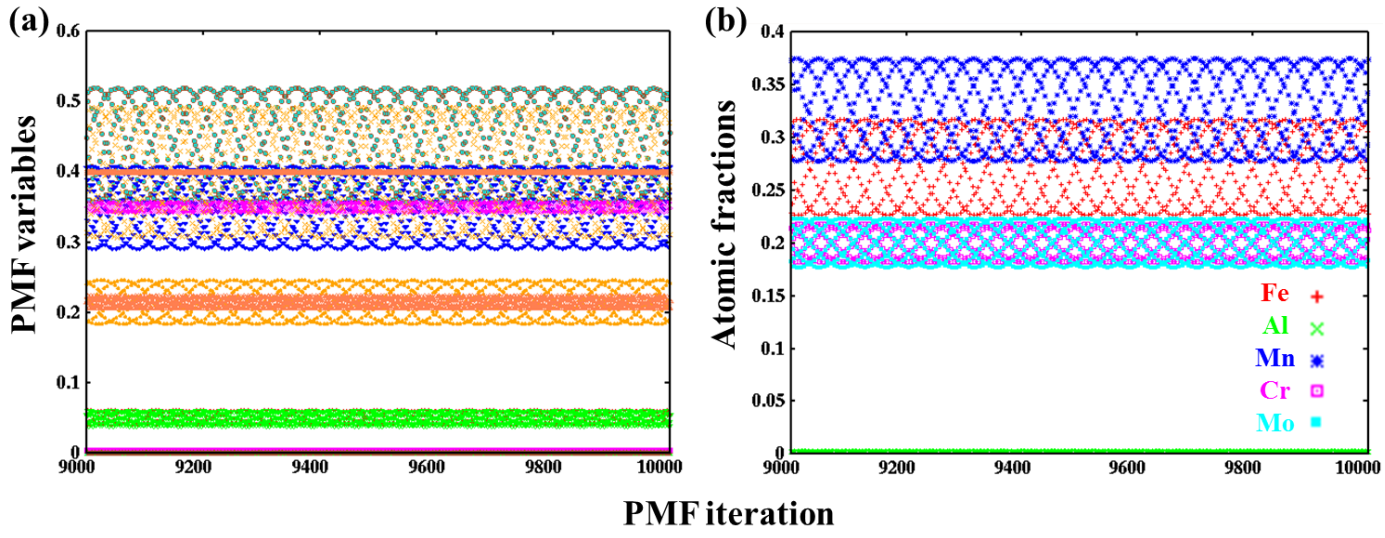

Figure 1: Typical oscillating behaviour of PMF algorithm over 1000 iterations, possibly occurring at low temperature (here AlCrFeMnMo at 600 K), as a consequence of the initial values chosen for PMF variables (set of 16 sublattice occupancies): (a) sublattice occupancies, (b) corresponding atomic fractions. On Fig. (a), the color code is immaterial,

various colors being used only to illustrate the oscillating behaviour of all PMF variables; on Fig. (b), red, green, deep blue, purple and cyan are used respectively for Fe, Al, Mn, Cr and Mo.

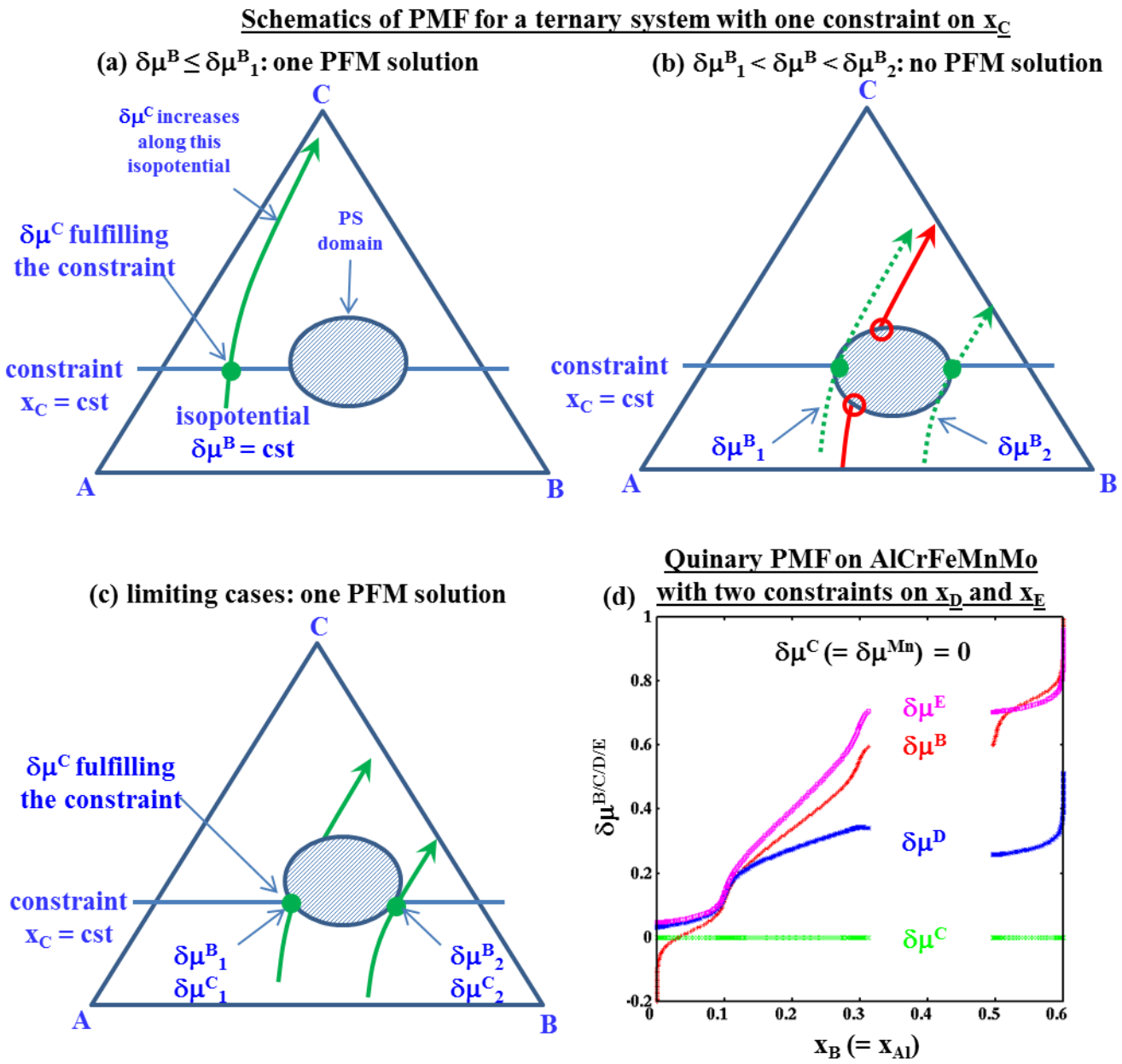

Figure 2: (a,b,c) For the simpler case of a ternary system with one constraint (constant x_C), schematic illustration of the relation between possibly oscillating constrained PMF and presence of PS domain: (a) most frequent situation (single-phase domain) yielding a PMF solution, (b) presence of PS domain, yielding no solution for the current B chemical potential $\delta\mu^B$, hence an oscillating behaviour for the PMF algorithm, (c) limiting cases with PMF solution ; (d) practical situation obtained for quinary PMF in AlCrFeMnMo with two composition constraints: constant-$\delta\mu^C$(= $\delta\mu^{Mn}$) isopotentials showing continuous $\delta\mu^B$ vs discontinuous ($\delta\mu^D$;$\delta\mu^E$).

RESULTS

General trends in MPEAs from PMF: long-range ordering and phase separation

AlCoCrFeNi

Following the same guidelines as in our previous MC study [13], we first focus on the general properties (i) and (ii), namely trends on long-range order (LRO) and phase separation (PS), as predicted from PMF, considering in turn 1) AlCoCrFeNi, 2) AlCrFeMnNi, 3) AlCrFeMnMo. As mentioned above, our approach conveniently provides, for decreasing temperatures, pseudo-ternary isothermal sections at fixed atomic fractions for a couple of chemical species (D and E in the notation of the Appendix) selected at convenience, respectively (Cr;Ni), (Mn;Ni) and (Cr;Mo) for the three systems listed previously. Our purpose being mainly to characterize and compare the behaviours of these systems in their typical HEA domain, i.e. around the equiatomic composition, this means choosing xD = xE = 1/5 as

constraints for our investigations and monitoring the behaviour around the center of the isothermal sections of the phase diagrams. The alloy composition on these pseudo-ternary isothermal sections can then be readily localized in the same way as done for true ternary diagrams, provided the sum of the three atomic fractions is equal to 1 – xD – xE.

Before turning to the description of the PMF results for these systems, a remark should be made about the practical identification of LRO states for MPEAs in simulations. In the bcc structure, distinguishing as usually four sublattices, the various kinds of LRO are well-known to be either B2, or $D0_3$ or B32 for binary alloys, together with $L2_1$ and XA as additional possibilities in ternary cases. Conversely, the LRO panorama becomes hardly tractable in higher-order systems such as quinary ones, owing to the drastically increasing number of possible combinations for the chemical species on the four sublattices. In this context, following previous MC simulation works [9,13], our investigations of LRO were simplified by restricting to a unique general B2-type kind of LRO, covering all these hardly classifiable possibilities, and considered to be the sole complementary case to the A2 solid solution. This approximate distinction between A2 disorder and B2-type LRO is sufficient for our purpose of characterizing overall LRO and PS trends, and these two MPEA states will be displayed respectively in red and black on all the phase diagrams presented below. For simplicity, this B2-type LRO will be abbreviated by B2 throughout.

The first system relevant for our investigations is AlCoCrFeNi, an interesting reference case since it made previously [9] the topic of experimental as well as simulation studies, both found in good agreement with each other. The isothermal sections of the PMF phase diagram for this system, obtained using the aforementioned 1NN pair energetics, and plotted for $x_{Cr} = x_{Ni} = 1/5$, are displayed on Figure 3.

As a general trend that nevertheless deserves recalling at first, the high-temperature A2 disordered solid solution (in red), found as expected to cover the whole isothermal section at high temperatures, is gradually replaced at temperature lowering by the B2-type LRO state (in black). The PMF calculations clearly illustrate (Figures 3a and 3b) that the LRO ordering process should propagate from the Al corner, the progressing front for the A2 → B2 transition remaining parallel to the Fe-Co axis. Interestingly, this transition appears to occur continuously in the composition plane, being associated with no two-phase domain. As shown on Figure 3a, LRO is predicted from PMF to reach the equiatomic point (green circle) roughly at T_{LRO} = 2000 K. This is recalled in Table 2, which collects the PMF characteristic LRO and PS temperatures for all alloys studied, together with their MC analogs reported from previous works. Table 2 also indicates that the MC value for T_{LRO} (admittedly exact value for the 1NN pair energetics currently used) was previously found to be around 1600 K, namely ~400 K above the PMF estimation. This feature - overestimation (for a given energy model, with respect to "exact" MC simulations) of LRO temperatures by several hundredths of K - is probably typical of PMF thermodynamics, as already noted previously [11].

The PMF approach also provides isopotential curves corresponding to constant Al and Co chemical potentials, which become visible at sufficiently low temperatures, e.g. 1000 K (Figure 3b). The gradually increasing curvature of these isopotential profiles in the LRO domain at the A2 / B2 "interface" suggests the emergence of a PS process, which becomes more evident at lower temperature (Figure 3c). This two-phase enclave growing exclusively within the LRO domain (while the A2 domain is only subjected to uniform shrinking parallel to the Fe-Co axis) is eventually found to reach the equiatomic composition at roughly 500 K. This is visible on Figure 3d, which also displays two constant-$\delta\mu^{Co}$ isopotentials delineating the PS domain around the equiatomic composition. Interestingly, the PS is found to be of mixed ordered / disordered A2 + B2 type, a feature in agreement with the conclusions of an earlier MC work [9,13] on the same system using the same energetics. One should however keep in mind that the isopotentials displayed on isothermal sections (Figure 3d) are not sufficient to infer the precise compositions of the phases occurring at PS, since in general, due to the constraints on x_D and x_E, $\delta\mu^D$ and $\delta\mu^E$ are not constant are discontinuous on either side of this domain along the isopotential (cf. also Fig. 2d).

	AlCoCrFeNi (equiat.)	AlCrFeMnNi (equiat.)	AlCrFeMnMo (equiat.)	AlCrFeMnMo (optim.)
T_{LRO} T_{PS}	2000 (1600) 500 (700 - 300)	1600 (1200) 500 (900 - 300)	1300 (1100) < 300 (900 - 300)	1300 (1000) < 300 (700 - 300)
B2-type compound	$[CoFeNi]_{\alpha\beta}[AlCr\{Fe\}]_{\gamma\delta}$ $([CoNi]_{\alpha\beta}[AlCrFe]_{\gamma\delta})$	$[\{Cr\}FeMnNi]_{\alpha\beta}[AlCr\{Mn\}]_{\gamma\delta}$ $([CrFeMnNi]_{\alpha\beta}[AlCrFeMn]_{\gamma\delta})$	$[AlCrMo]_{\alpha\beta}[\{Cr\}FeMn]_{\gamma\delta}$ $([AlCrMo]_{\alpha\beta}[CrFeMn]_{\gamma\delta})$	$[AlCrMo]_{\alpha\beta}[\{Cr\}FeMn]_{\gamma\delta}$ $([AlCrMo]_{\alpha\beta}[FeMn]_{\gamma\delta})$

Table 2: From PMF phase diagrams, approximate calculated transition temperatures (K) of long-range ordering (LRO) and phase separation (PS) for the various MPEA systems considered in this work, including comparison with earlier MC estimations (the latter between parentheses, taken from Refs. [9] for AlCoCrFeNi and [13] for other alloys). For AlCrFeMnMo, the "optimized" experimental alloy has composition Al22Cr22Fe29Mn20Mo7. In the table, MC estimations of T_{PS} are given in a range of temperatures, the upper bound of which corresponds to typical « dispersed two-phase systems » [13] appearing in MC simulations, while the lower bound refers to well-separated two-phase mixtures. The last row provides the PMF formula for the single-phase B2-type compound occurring below T_{LRO} in each case, together (between parentheses) with MC predictions recalled from the same earlier works [9,13]. {} symbols indicate those species for which non negligible though minor sublattice occupancies were found in PMF.

As another interesting remark, it is also a known fact from previous works (e.g. Ref. [11]) that PMF may significantly underestimate, or even completely overlook, PS domains. Contrary to LRO, this discrepancy is however not clearly suggested by Table 2, which reports that a PS temperature range between 300 K and 700 K was previously inferred from MC simulations. Indeed, as emphasized previously [13], interpretation of the PS behaviour in MC simulations is made more intricate by the seemingly progressive rise of PS when temperature decreases. This entails the existence, in a temperature range extending over several hundredths of K, of an intermediate state, referred to previously as a "two-phase dispersed system" (TPDS), and possibly an artefact typical of MC simulations, due to interfacial effects (coherent interfaces) in close relation with the precise kind of energetics used. The upper and lower bounds of the MC temperature range for PS (as recalled in Table 2) respectively correspond to the emergence of this TPDS and unambiguous identification of a PS system including a sharp interface. While our purpose here is not to discuss this issue further, it is worth mentioning that these ambiguities on PS are overcome in PMF, a noticeable advantage of the latter and related (CVM) approaches. On the whole, and taking into account these MC uncertainties, the agreement between MC and PMF on the PS temperature predicted for equiatomic AlCoCrFeNi can be considered as acceptable, indicating that PS in this system should take place at moderate temperatures.

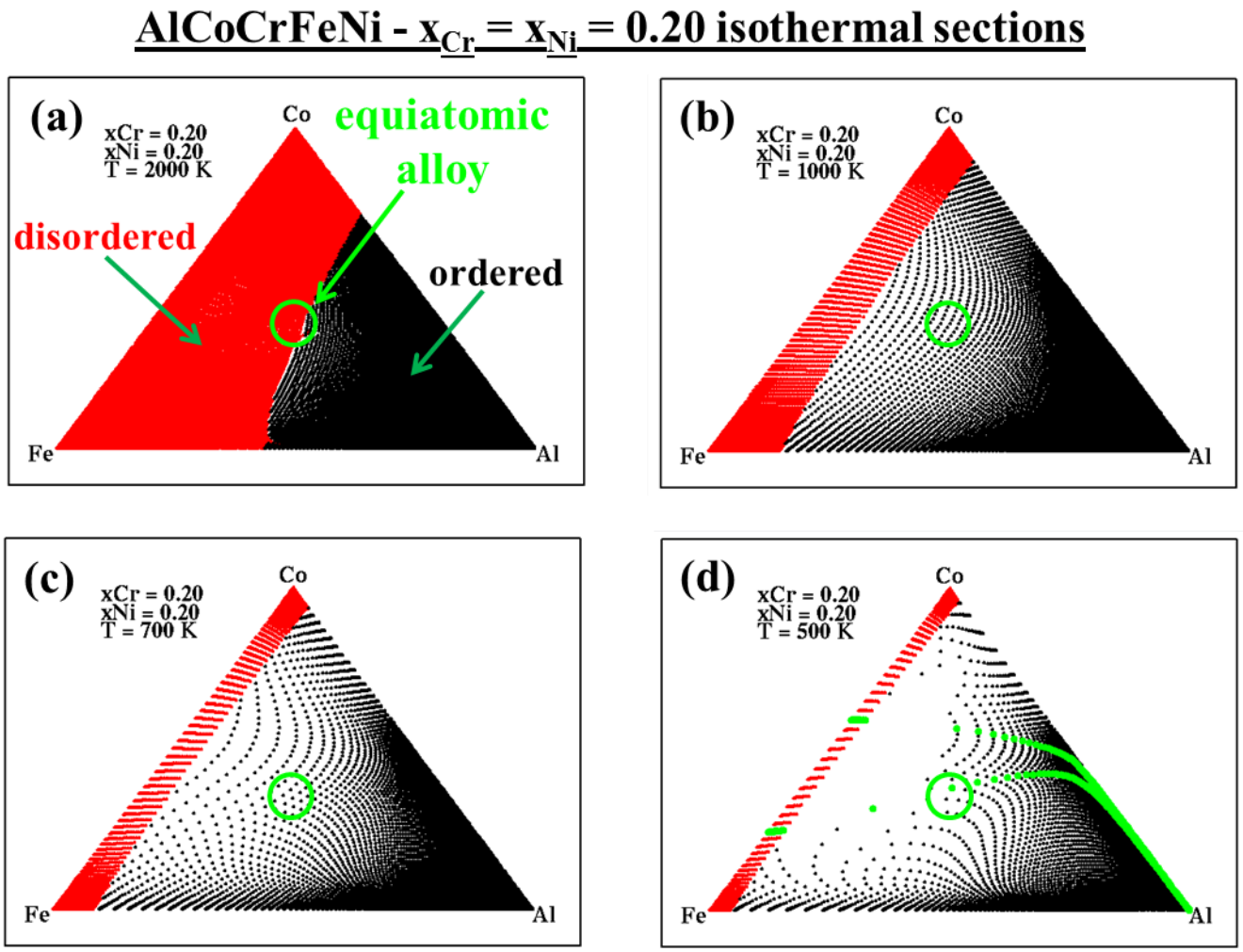

Figure 3: PMF phase diagram of bcc AlCoCrFeNi including the equiatomic alloy (isothermal sections for $x_{Cr} = x_{Ni} = 1/5$) at several decreasing temperatures: (a) temperature for which the equiatomic alloy lies on the A2 / B2 second-order transition line; (b,c) intermediate temperatures illustrating the shrinking of the A2 domain ; (d) temperature for which the equiatomic alloy lies reaches a phase-separation domain. The disordered (A2) and ordered (B2-type) domains are displayed in red and black respectively. The green circle sketches the equiatomic alloy. The green points on Figure (d) indicate two constant-$\delta\mu^{Co}$ isopotentials delineating the A2 + B2 PS domain.

AlCrFeMnNi

As a further step to get better insight into the merits of PMF for MPEA thermodynamics, it is relevant to consider the AlCrFeMnNi system, deduced from AlCoCrFeNi by substituting Co with Mn. For the energy model in its initial form H^{ij} (Table 1), this shift of quinary system amounts to replacing Co-X interactions by Mn-X ones. Before turning to PMF, it is instructive to have a closer look at this point, which can be done using Figure 4, displaying only those interactions concerned by the change of chemical element. The strongest effect of this change is clearly related to the replacement of the strongly attractive Al-Co interaction by the more moderate, also attractive, Al-Mn one, while other

interactions relevant to the Co →Mn substitution appear to be much less modified. This difference between both alloys should thus be mostly visible by comparing isothermal sections performed in the AlCoFe and AlFeMn planes, but we did not verify this point, since it is not essential in the present study.

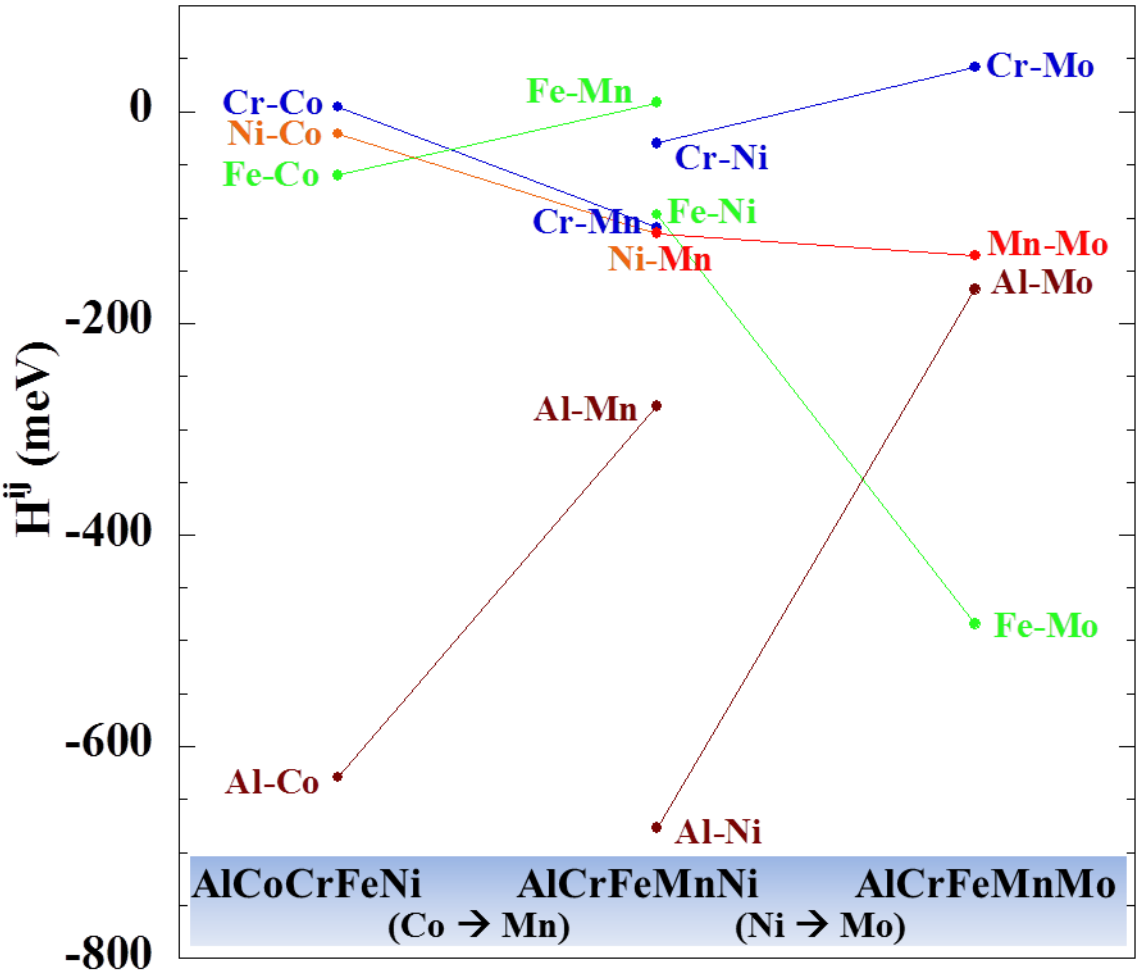

Figure 4: Evolution of pair enthalpy parameters H^{ij} (from Ref. [12]) along the AlCoCrFeNi → AlCrFeMnNi → AlCrFeMnMo sequence.

Turning then to PMF thermodynamics for AlCrFeMnNi, Figure 5 displays various isothermal sections of the phase diagram, plotted in the AlCrFe plane with constraints $x_{Mn} = x_{Ni} = 1/5$ chosen to encompass the equiatomic alloy. Firstly, in agreement with the previous remarks on H^{ij} parameters (though such connections should be handled carefully, since the whole thermodynamic behaviour can obviously not be inferred fully from inspection of H^{ij} values), the overall trends for this system, at least under the composition constraints specified, look similar to those noted previously for AlCoCrFeNi. In particular, Figure 5a clearly shows that the onset of LRO at cooling is expected to arise prior to PS in the equiatomic alloy. Here again, the absolute value of T_{LRO} from PMF for this specific alloy should not be regarded as reliable. However, comparison between equiatomic AlCoCrFeNi and AlCrFeMnNi should be allowed (Table 2), and the A2 → B2 transition temperature for AlCrFeMnNi (~1600 K) is found to be significantly lower than in AlCoCrFeNi. Moreover, confronting these PMF values with their MC counterparts (also from Table 2) confirms, at least to a certain extent, that PMF can indeed be used to compare LRO trends in two distinct MPEAs. This conclusion should nevertheless be checked more thoroughly, by PMF inspection of a larger number of MPEA systems and alloys. Therefore, provided the 1NN pair energetics in Table 1 is valid, these results for T_{LRO} point out for (equiatomic) AlCrFeMnNi a better HEA behaviour than for (equiatomic) AlCoCrFeNi, namely the former alloy remains in A2 disordered state at lower temperatures, a conclusion that should be easily checked experimentally.

The second major trend (ii) in AlCrFeMnNi is illustrated on Figures 5(b-d), showing that the onset of PS occurs along the A2 / B2 phase separation boundary, in a way very similar to AlCoCrFeNi, leaving an A2 + B2 two-phase system. This PMF prediction is in agreement with previous MC results using the same energy model (cf. Table 2 in Ref. [13]), which also pointed out that PS should be of mixed ordered / disordered A2 + B2 type for both equiatomic AlCoCrFeNi and AlCrFeMnNi. The typical PS temperatures from PMF are found quite similar (~500 K) in both alloys, a conclusion which also roughly agrees with MC simulations (Table 2). While the comparison PMF / MC is made difficult here due to the aforementioned TPDS, it seems however reasonable to assume that phase separation is expected at rather low temperature in both MPEAs. It would certainly be interesting to investigate other quinary

systems, in order to try to identify other (groups of) MPEAs displaying strongly different behaviours (PS prior to LRO…). Therefore, summarizing our PMF conclusions for AlCoCrFeNi and AlCrFeMnNi, it seems reasonable to assume that PMF can indeed be employed, rather than much more computationally demanding MC full simulations, to explore at least 1) the succession of LRO and PS phenomena at cooling, and 2) the kind of two-phase system (purely disordered A2 + A2'? purely ordered B2 + B2'? mixed ordered / disordered A2 + B2?) emerging at PS, possibly together with 3) comparison of characteristic temperatures T_{LRO} and T_{PS} between two MPEA systems.

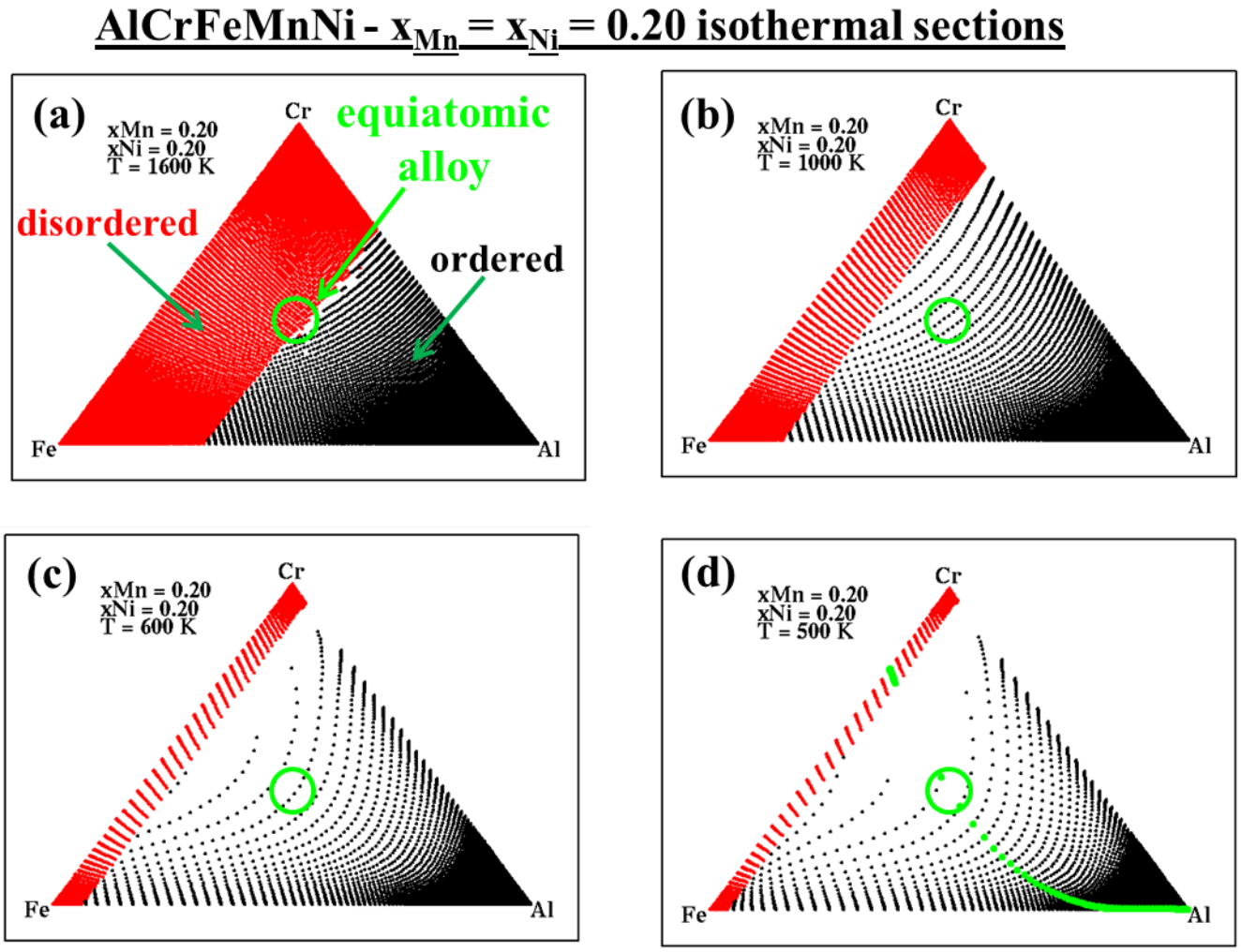

Figure 5: same as Figure 3, for bcc AlCrFeMnNi including the equiatomic alloy (isothermal sections for $x_{Mn} = x_{Ni} = 1/5$). The disordered (A2) and ordered (B2-type) domains are displayed in red and black respectively.

AlCrFeMnMo

Considering now AlCrFeMnMo, of primary interest owing to the lack of results on this quinary system, it is relevant to focus more thoroughly on two compositions, namely the equiatomic alloy and a heuristically "optimized" alloy with composition Al22Cr22Fe29Mn20Mo7, both of which were extensively studied elsewhere from experiments [6] and MC simulations using the same 1NN pair energetics [13]. As previously, this system can be regarded as deduced from AlCrFeMnNi by substituting Ni with Mo, and the energy parameters concerned by this substitution are plotted on Figure 4. While for Al the Ni →Mo substitution roughly has the same effect (reduced attractive interaction) as the previous Co → Mn one, its overall influence on alloy energetics is probably made more intricate by an opposite effect (enhanced attraction) on Fe, together with a change of sign of the interaction with Cr which becomes repulsive. From these H^{ij} trends, it however seems difficult to draw reliable conclusions about the compared thermodynamic properties of AlCrFeMnNi and AlCrFeMnMo, which further justifies the current PMF approach.

Turning then to the PMF phase diagrams of AlCrFeMnMo, a set of isothermal sections relevant for the equiatomic alloy, namely under constraints $x_{Cr} = x_{Mo} = 1/5$, are displayed on Figure 6. The A2 / B2 transition line in the AlFeMn plane is found to lie parallel to the Al-Mn axis, while LRO is first visible around the Fe corner of the pseudo-ternary AlFeMn isothermal cut, these features contrasting with AlCoCrFeNi and AlCrFeMnNi studied previously, the latter being characterized by the A2 / B2 line parallel to Fe-Co or Fe-Cr axis (resp.) and LRO ordering emerging around the Al corner. This difference illustrates the intricacy of the predicted thermodynamic properties in MPEAs, even within the seemingly simple frame of 1NN pair interactions. Figure 6a points out $T_{LRO} \sim 1300$ K for equiatomic AlCrFeMnMo, a value lying here again roughly 200 K above its counterpart deduced from MC simulation (Table 2).

In AlCrFeMnMo, the shrinking of the A2 domain at cooling occurs somewhat differently from noted in the previous couple of systems, and subsists at last around the Mn corner. In possible connection with this more limited A2 domain, PS in AlCrFeMnMo is not found to start along the A2 / B2 line, but instead near the Al corner and within the B2-type domain (Figure 6c). In spite of this discrepancy, Figure 6c also indicates that the temperature range for PS occurrence, namely 500 - 600 K, is similar in AlCrFeMnMo, AlCoCrFeNi and AlCrFeMnNi. It is interesting to note the reasonable agreement on these PMF trends with previous MC conclusions, since in the latter PS was found to lead to a mixture of two B2-type phases, a conclusion in line with Figure 6c. While the opening of the PS domain is clearly visible on Figures 6c and 6d, the latter pertaining to low temperature (300 K) also displays an example of PMF artifact As mentioned in the previous section, such an artifact is due to the lack of convergence of the PMF algorithm, and induces missing points that however should not be interpreted as PS. Finally, it may be recalled here that comparison between PMF and MC for PS is made less significant in AlCrFeMnMo by the fact that the precise value of T_{PS} is difficult to determine from the MC profiles of LRO parameters of pair correlation functions [13], as soon as phase separation starts to occur, due to the systematic existence in a non-negligible temperature range, of an TPDS state systematically obtained for all alloys and possibly an artifact due to spurious coherent interface effects unavoidable in MC simulations while overcome in MF analytical approaches.

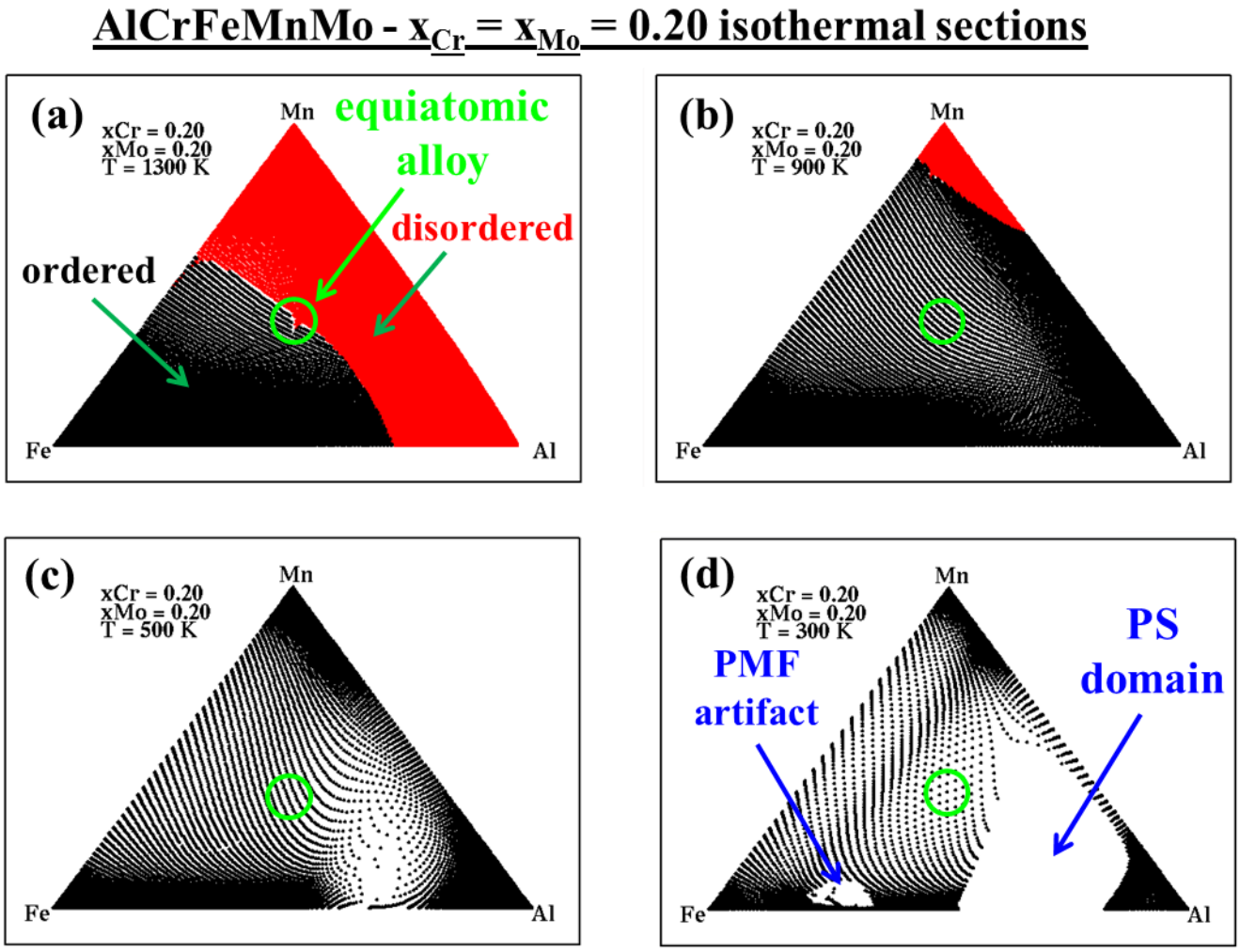

Figure 6: same as Figure 3, for bcc AlCrFeMnMo including the equiatomic alloy (isothermal sections for $x_{Cr} = x_{Mo} = 1/5$). The disordered (A2) and ordered (B2-type) domains are displayed in red and black respectively.

To complete the present PMF comparative investigations of MPEAs, we now consider the effect of a moderate composition change in AlCrFeMnMo, leading to an Fe-enriched Mo-depleted alloy Al22Cr22Fe29Mn20Mo7 previously selected from heuristic optimization [6]. This "optimized alloy" can also be explored conveniently with PMF, using isothermal sections under the constraints x_{Cr} = 22 % and x_{Mo} = 7 % (Figure 7). In order to facilitate comparison between the equiatomic and optimized cases, the temperatures used to draw these sections are the same in both cases. From Figs. 7a and 6a, this choice appears to be consistent with the fact that the temperature for LRO emergence was found in PMF to be almost the same ~ 1300 K in both alloys. This PMF behaviour is in agreement with earlier MC results (Table 2), and further confirms the general trend, already expected from previous works [11] and noted throughout in the four MPEAs studied here, that PMF yields ~ 200 – 300 K systematic overestimations of T_{LRO}. When analyzing the somewhat larger effect of composition change of T_{LRO} visible in MC than in PMF, it should also be kept in mind, as demonstrated in earlier works [9,13], that MC estimations of T_{LRO}, though less critical than

noted for T_{PS}, are not free from uncertainties, and MF approaches are thus more accurate in this respect. This point will be further illustrated below. As another noticeable feature, confronting Figs. 7a and 7b with their equiatomic analogs shows that the selected composition change has a significant influence on the A2 → B2 transformation at cooling, the LRO phase in the optimized alloy emerging from the middle of the Al-Fe axis, instead of the Fe corner in the equiatomic case. Moreover, instead of a single zone located along the Al-Mn axis and shrinking around the Mn corner, the A2 domain in the optimized case gradually subdivides into two areas around the Mn and Al corners. Remarkably, for all MPEAs considered in the present study, PMF calculations suggest that the A2 domain at cooling should last subsist near edges or corners of the composition space, thus at odds with the common assertion that disordered A2 should be mostly favoured, for entropy reasons, around the center (equiatomic case) of this space. Comparison of Figs. 7c and 6c also allows to estimate the influence of the selected composition change on PS trends, showing a clear discrepancy, since in contrast with the equiatomic case, no PS is detected at 500 K in the optimized one. The emergence of a PS domain in the latter case starts only at low temperature (300 K, Fig. 7d), whereas for the same temperature a large domain is already opened within the equiatomic section. In addition, in both composition domains, PS is found to occur mostly near the Al corner, the alloy previously selected as optimized (green circle) being therefore not concerned with this process even at low temperatures.

Most remarkably, gathering the above results for the set of four MPEAs studied allows to conclude that PMF, within a given 1NN pair interaction model, should provide a handsome and reasonably reliable way to characterize, with moderate computational requirements, any MPEA as concerns trends of (i) LRO and (ii) PS, ensuring an easy survey across the whole composition space. While the PMF formalism can be extended without difficulty to include 2NN interactions, no investigations of the influence of these additional parameters have been carried out so far. Finally, from PMF thermodynamics built on the current 1NN energetics, we must also conclude that, around the equiatomic domain, the AlCrFeMnMo should phase-separate only at relatively low temperature, and within the B2-type ordered domain, a conclusion seemingly at odds with the experimental observations [6] of AlCrFeMnMo samples, pointing out two bcc phases with distinct compositions and no long-range order.

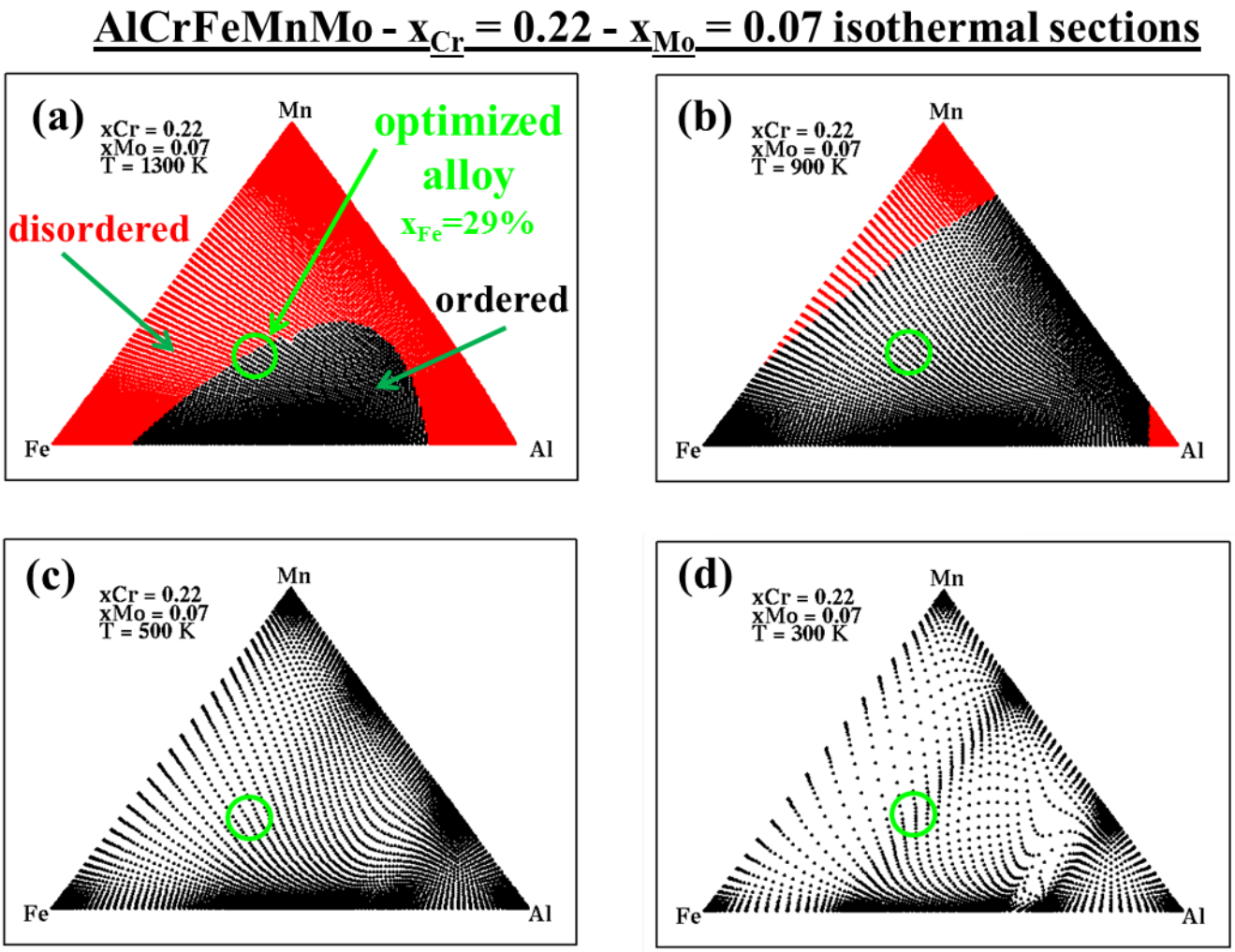

Figure 7: same as Figure 6 (AlCrFeMnMo system), for an isothermal section (x_{Cr} = 22% ; x_{Mo} = 7 %) including the alloy selected as "optimized" for experiments [6]. The composition of this optimized alloy is delineated by the green circle. The disordered (A2) and ordered (B2-type) domains are displayed in red and black respectively.

Site occupancies in LRO states

To conclude this PMF study of MPEAs, we now investigate, for the same alloys, the PMF predictions about somewhat more subtle (i.e. more difficult to assess experimentally than LRO and PS) trends, namely sublattice occupancies in LRO phases. It should be noticed first that the present PMF approach does not easily allow to reach the composition of each phase (a fortiori the sublattice occupancies of LRO phases) in PS domains, because the handling of isothermal cuts at constant x_D and x_E entails discontinuous D and E chemical potentials on either side of the domain. We therefore mainly restrict our analysis to the single-phase LRO state occurring just below T_{LRO} at the A2 → B2 transition, and consider the same compositions as previously, i.e. equiatomic AlCoCrFeNi and AlCrFeMnNi, together with equiatomic and optimized AlCrFeMnMo. The profiles of sublattice occupancies for A2 → B2 transitions at cooling across T_{LRO} are displayed on Figures A1 to A4 provided in appendix. The results are summarized in the last row of Table 2, which provides the formula of the B2-type compound as predicted from PMF for each MPEA, together with its MC counterpart reported from a previous work [9,13].

For AlCoCrFeNi, the occupancy profiles indicate T_{LRO} = 1820 K (Fig. A1), in better agreement with MC results than previously obtained from the phase diagram analysis. The B2-type ordered phase from PMF is $[CoFeNi]_{\alpha\beta}[AlCr\{Fe\}]_{\gamma\delta}$, also in satisfactory agreement with MC (Table 2), except Fe found in MC to occupy more selectively a single cube shared with Al and Cr. This slight discrepancy may be due to the fact that the PMF analysis (Fig. A1) is focused around T_{LRO}, for which Fe is still randomly distributed, while the Fe occupancy becomes more selective at lower temperatures [9]. For AlCrFeMnNi, the occupancy profiles (Fig. A2) indicate that T_{LRO} = 600 K, confirming the previous estimation from the phase diagram. The B2-type ordered phase found in PMF, i.e. $[\{Cr\}FeMnNi]_{\alpha\beta}[AlCr\{Mn\}]_{\gamma\delta}$, agrees reasonably with earlier MC simulations pointing out nearly random distributions for Cr, Fe and Mn, anly Ni and Al being concerned with B2-type order. As concerns AlCrFeMnMo, the occupancy profiles of Figs. A3 and A4 show that the B2-type ordered phase from PMF both for the equiatomic and optimized alloys is $[AlCrMo]_{\alpha\beta}[\{Cr\}FeMn]_{\gamma\delta}$, which agrees reasonably with MC simulations, except a more random Cr behaviour predicted in the latter approach for the equiatomic case. The PMF occupancy profiles also confirm close values for T_{LRO} ~1300 K in both AlCrFeMnMo alloys, while MC simulations rather suggest that the equiatomic → optimized change may entail a T_{LRO} decrease by ~ 100 K. On the whole, this brief analysis of sublattice occupancies in MPEAs near the single-phase A2 → B2 transition further illustrates that PMF approaches provide quite reliable conclusions, and thus may indeed be useful to investigate MPEA thermodynamics in the context of pair energy models.

DISCUSSION

The purpose of the present work was to illustrate the use of the PMF approach to investigate the thermodynamic properties of MPEAs. We hope that the above results demonstrate that, in spite of its relative simplicity, this framework is able to provide useful information about the effect of composition changes in a given MPEA, or about the influence of modifying the MPEA system itself through the replacement of an element with another one. While subtle features of MPEA mixtures may lie beyond its scope of validity, the few examples handled in this work suggest that PMF should offer a convenient route to explore more general MPEA trends, of wide practical importance, especially those concerned with long-range ordering and phase separation. As another advantage, the approach delineated here provides an easy way to take benefit from nowadays increasingly available ab initio-built energy databases, such as the one employed for our calculations [9,12]. Such databases offer the opportunity to build quickly a large number of model alloys involving various elements, which can then be conveniently employed, due to the good capabilities of PMF for investigations, in particular as regards exploring the huge composition space of MPEAs. It is also worth noting here that the current approach could be straightforwardly transposed to fcc-based MPEAs, the easily reachable PMF free energy allowing then to explore bcc-fcc equilibria and competitions.

Although this context is rather encouraging, a first issue deserving discussion concerns the use of simple, possibly oversimplified, short-range pair energy models to build PMF thermodynamics. This was not our purpose here to explore the validity of such models for MPEAs. Our ambition was more moderate, our study being justified by the availability of such models in the literature, and by the fact that these models may be given some credit because they were derived from large sets of ab initio calculations. For instance, justifying the use of extended databases of compound formation energies to build effective first-nearest-neighbour pair energy parameters (those used above) between various (~30) chemical elements constitutes a challenging issue in itself. In the longer term, justifying – or discarding – such energy models may be achieved by testing their merits for thermodynamic modelling of MPEAs. This in turn could be carried out by performing a sufficient amount of (PMF or MC) simulation studies on various MPEA systems, along the same lines as described above for a small panel of systems, together with dedicated reference experiments on these MPEAs, for which well equilibrated states should be elaborated and characterized. On the whole, this work has hardly been done so far.

Another issue worth discussing, in close connection with our work, concerns the hypothesis of pair interactions restricted to first-nearest neighbours (1NN) when studying MPEAs in a given (body-centered or face-centered) cubic

structure. This restriction, which is at the core of the energy database currently available [12] and used above, may seem somewhat at odds with the abundant literature on alloy modelling [10], which usually includes, at least, the first two neighbour shells, a minimum requirement, in order for pair models to distinguish between the various kinds of order frequently observed in alloys with bcc or fcc structures, mostly common in the field of MPEAs. Here again, in the present state of our knowledge, it seems difficult to estimate how critical this restriction is, if we intend to explore MPEA thermodynamics. In particular, while more subtle kinds of order (B32, $L2_1$, XA,…) are necessarily overlooked in the 1NN restriction, it is not clear whether this simplification is to modify strongly the predictions of modelling as regards "coarser" properties, such as the onset of long-range order or phase separation in an MPEA solid solution. Therefore, when considering such properties, the validity and merits of the 1NN pair approximation for (cubic) MPEAs still constitute a largely open issue, which could be investigated in more detail. For instance, in the present work, owing to the agreement noted previously on AlCoCrFeNi and AlCrFeMnNi, the discrepancy between experimental and modelling conclusions on AlCrFeMnMo appeared rather surprising, and this may raise the question of the validity of the 1NN approximation for pair interactions involving Mo. While the PMF easily lends itself to include 2NN, such investigations with up-to-2NN PMF were not carried out, because this would have raised the issue of properly choosing the 2NN energy parameters Mo-X (X = Al, Cr, Fe, Mn in our case), a non-straightforward task, since this choice is expected to modify in turn the effective 1NN parameters. Moreover, the relevance of including 2NN may be questioned in itself, since one cannot exclude some failure of the 1NN energy parameters involving Mo as provided in the current database in of 1NN energy parameters in H^{ij} form.

Our work also points out questions about the inherent weaknesses of PMF, since this approach remains a rather crude approximation for the alloy entropy. The requirement being to preserve the advantages (efficiency and flexibility) of analytical formulations with respect to more cumbersome MC simulations, this logically suggests to discuss the possibility of converting the above PMF formulation into the more sophisticated and accurate format offered by the cluster variation method (CVM), in particular within the tetrahedron approximation well suited for cubic alloys. Within the usual grand canonical framework of CVM, this extension should raise no difficulty. However, the issue is made slightly more intricate by the appealing requirement to preserve the aforementioned constrained formulation for PMF, since this allows to obtain easily tractable pseudo-ternary isothermal sections of phase diagrams in quinary (or even higher-order) MPEAs. More precisely, this is related with the technical issue of exploring the compatibility between the constrained procedure successfully employed for PMF and the "natural iteration" algorithm (efficiently converging and avoiding more sophisticated, often less stable, procedures) used in tetrahedron CVM. This task could provide an interesting topic for future works, which may lead to an efficient tool to investigate thermodynamics of MPEAs from pair models, Achievement here may allow to increase significantly the accuracy level of thermodynamic characterization of a given 1NN or 1NN-2NN pair energy model, since tetrahedron CVM is recognized as a remarkably accurate method, an interesting feature confirmed by direct MC simulations in a recent work on atomic-scale modelling of Mn steels [11].

CONCLUSION

In this work, we developed and applied an original "composition-constrained" point mean-field (PMF) approach designed to explore efficiently the thermodynamic properties of multi-principal-element alloys (MPEAs). Its efficiency was demonstrated by application to the AlCoCrFeMn → AlCrFeMnNi → AlCrFeMnMo sequence of systems, which allowed exploring exhaustively two key-issues, namely (i) long-range ordering (LRO) and (ii) phase separation (PS), both of primary importance when searching for MPEAs with good properties. As a noticeable advance, our approach offers a convenient way to get a quick at-a-glance survey of LRO and PS in many MPEAs over the whole composition space, and thus to easily compare various MPEAs as regards these trends. These advantages make PMF a useful complementary tool with respect to more accurate but much more cumbersome Monte-Carlo "full" simulations, the latter being often restricted to selected compositions due to their high computational cost. In conjunction with reference experiments, more extended applications of our PMF approach to wider panels of multi-element systems may help identifying useful features as guidance rules for alloy design, and suggest improvements for the energy models nowadays available for MPEAs. Transposition of the current PMF formalism towards the more accurate cluster variation method may also provide a useful extension of this work.

BIBLIOGRAPHY

[1] High-Entropy Alloys - Fundamentals and Applications, M. C. Gao, J.-W. Yeh, P. K. Liaw, Y. Zhang (Editors), Springer (2016)

[2] A novel ultrafine-grained high entropy alloy with excellent combination of mechanical and soft magnetic properties, C. Chen, H. Zhang, Y. Fan, W. Zhang, R. Wei, T. Wang, T. Zhang, F. Li, J. Magn. Magn. Mater. 502, 5 (2020)

[3] Effects of Cu and Zn on microstructures and mechanical behavior of the medium-entropy aluminum alloy, B. Zhang, P.K. Liaw, J. Brechtl, J. Ren, X. Guo, Y. Zhang, Journal of Alloys and Compounds 820, 153092 (2020)
[4] On the enhanced wear resistance of CoCrFeMnNi high entropy alloy at intermediate temperature, J. Joseph, N. Haghdadi, M. Annasamy, S. Kada, P.D. Hodgson, M.R. Barnett, D.M. Fabijanic, Scripta Mater. 186, 230 (2020)
[5] High Entropy Alloys - Innovations, Advances and Applications, T. S. Srivatsan, M. Gupta (Editors), CRC Press (2020)
[6] Novel Multicomponent Powders from the AlCrFeMnMo Family Synthesized by Mechanical Alloying, T. Stasiak, S. N. Kumaran, M. Touzin, F. Beclin, C. Cordier, Adv. Eng. Mater. 21, 1900808 (2019)
[7] Understanding phase equilibria in high-entropy alloys: I. Chemical potentials in concentrated solid solutions – Atomic-scale investigation of AlCrFeMnMo, R. Besson, J. Alloys and Compounds 872, 159745 (2021)
[8] Understanding phase equilibria in high-entropy alloys: II. Atomic-scale study of incorporation of metallic elements in Cr carbides – Application to equilibrium with AlCrFeMnMo, R. Besson, J. Alloys and Compounds 874, 159959 (2021)
[9] Predictive multiphase evolution in Al-containing high-entropy alloys, L. J. Santodonato, P. K. Liaw, R. R. Unocic, H. Bei, J. R. Moris, Nat. Commun. 9, 4520 (2018)
[10] Order and phase stability in alloys, F. Ducastelle, North-Holland (1991)
[11] Ab initio thermodynamics of complex alloys: the case of Al- and Mn-doped ferritic steels, R. Besson, J. Dequeker, L. Thuinet, A. Legris, Acta Materialia 169, 284-300 (2019)
[12] Criteria for predicting the formation of single-phase high-entropy alloys, M. C. Troparevsky, J. R. Morris, P. R. C. Kent, A. R. Lupini, G. M. Stocks, , Physical Review X 5, 011041 (2015)
[13] Atomic-scale modeling of structural phase transformations in AlCrFeMnMo high-entropy alloys during thermal treatments, W. Sekkal, R. Besson, A. Legris, J. Alloys and Compounds 876, 160201 (2021)
[14] Configurational entropy in multicomponent alloys: matrix formulation from ab Initio based Hamiltonian and application to the FCC Cr-Fe-Mn-Ni system, A. Fernández-Caballero, M. Fedorov, J. S. Wróbel, P. M. Mummery, D. Nguyen-Manh, Entropy 21, 68 (2019)
[15] Chemical short-range order in derivative Cr–Ta–Ti–V–W high entropy alloys from the first-principles thermodynamic study, D. Sobieraj, J. S. Wróbel, T. Rygier, K. J. Kurzydłowski, O. El Atwani, A. Devaraj, E. Martinez, D. Nguyen-Manh, Phys. Chem. Chem. Phys. 22, 23929 (2020)

Appendix:
Sublattice occupancies across the single-phase A2→ B2 transition in MPEAs from PMF calculations

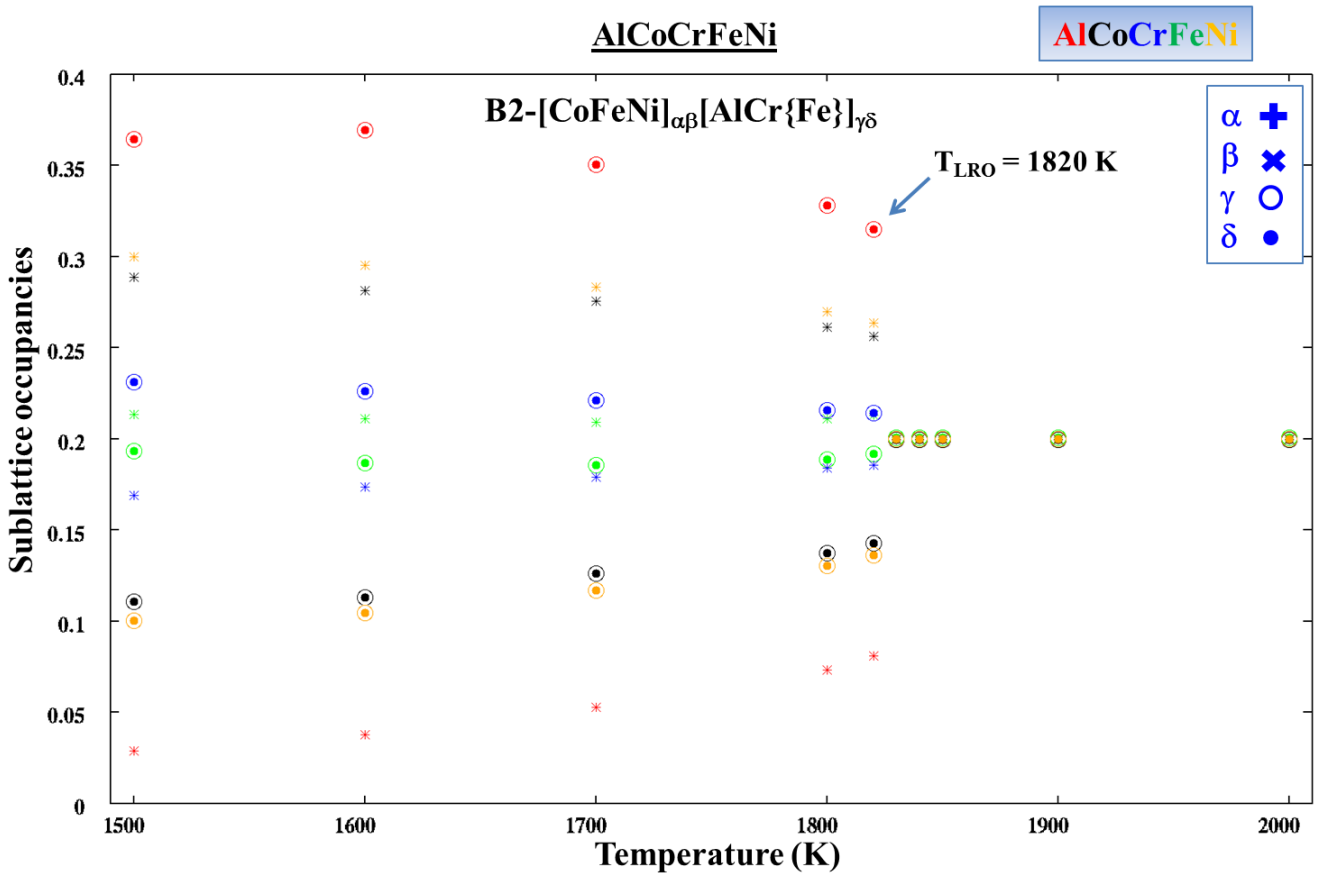

Figure A1: From current PMF calculations, evolution of sublattice occupancies with temperature for each chemical species in equiatomic AlCoCrFeNi.

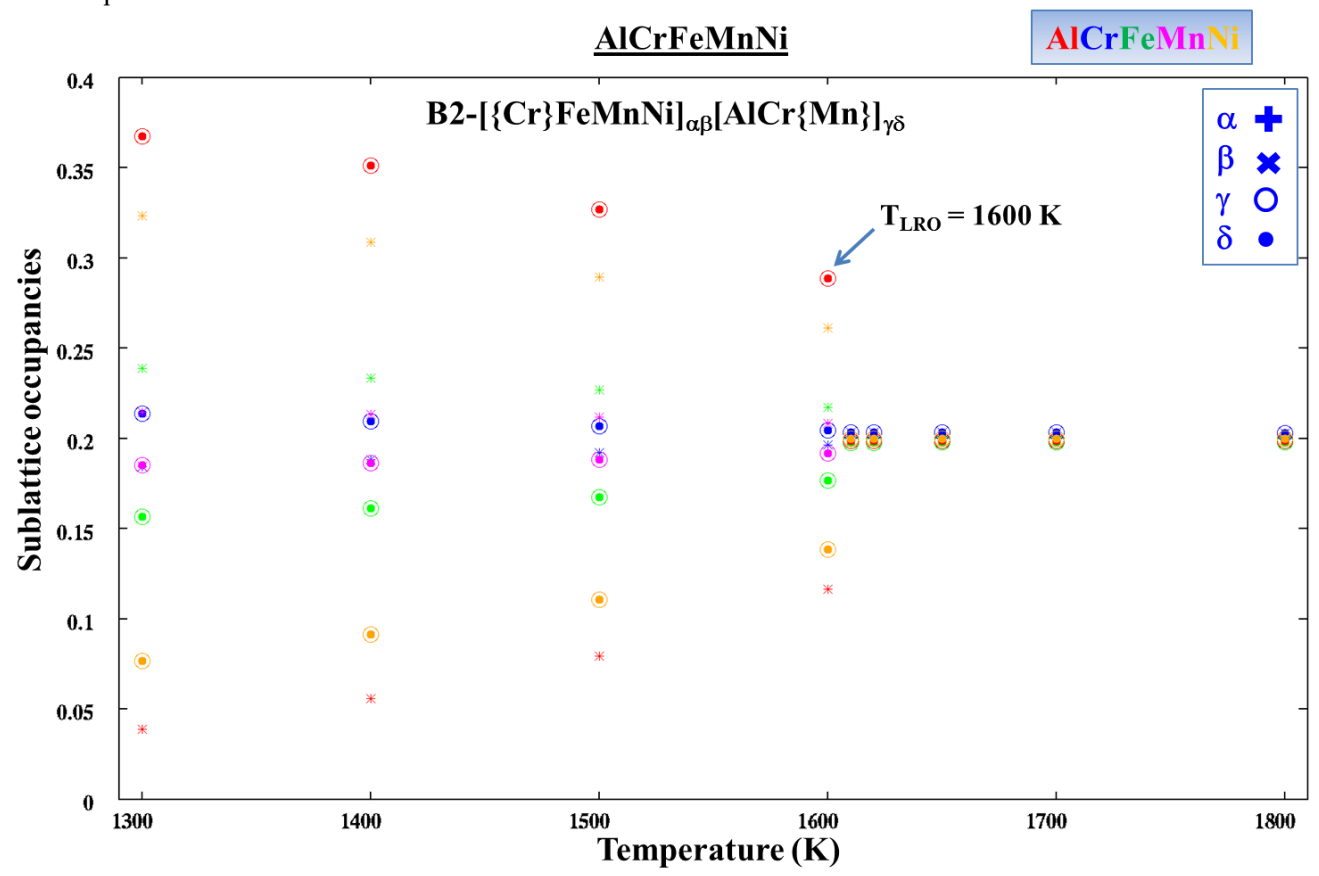

Figure A2: Same as Fig. A1, for equiatomic AlCrFeMnNi.

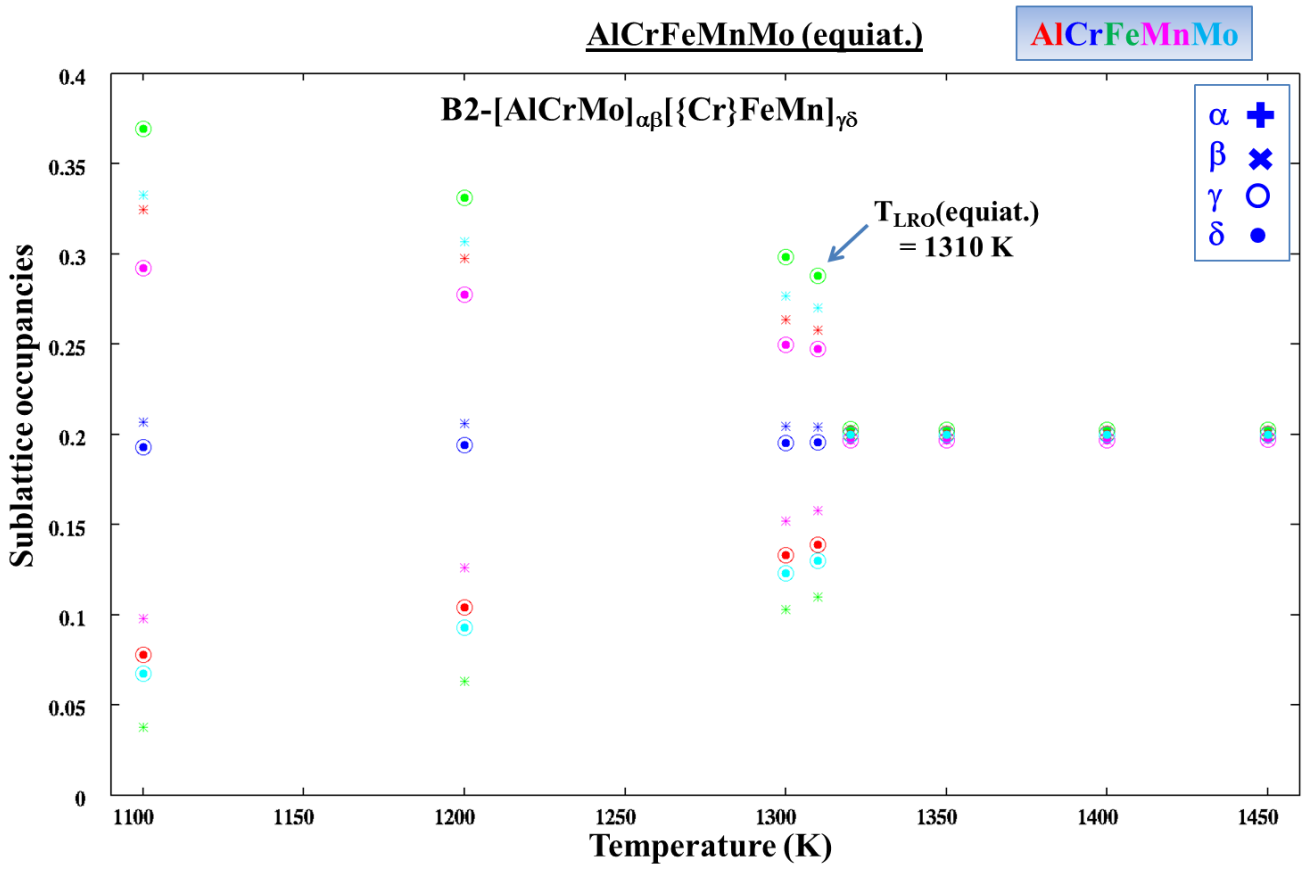

Figure A3: Same as Fig. A2, for equiatomic AlCrFeMnMo.

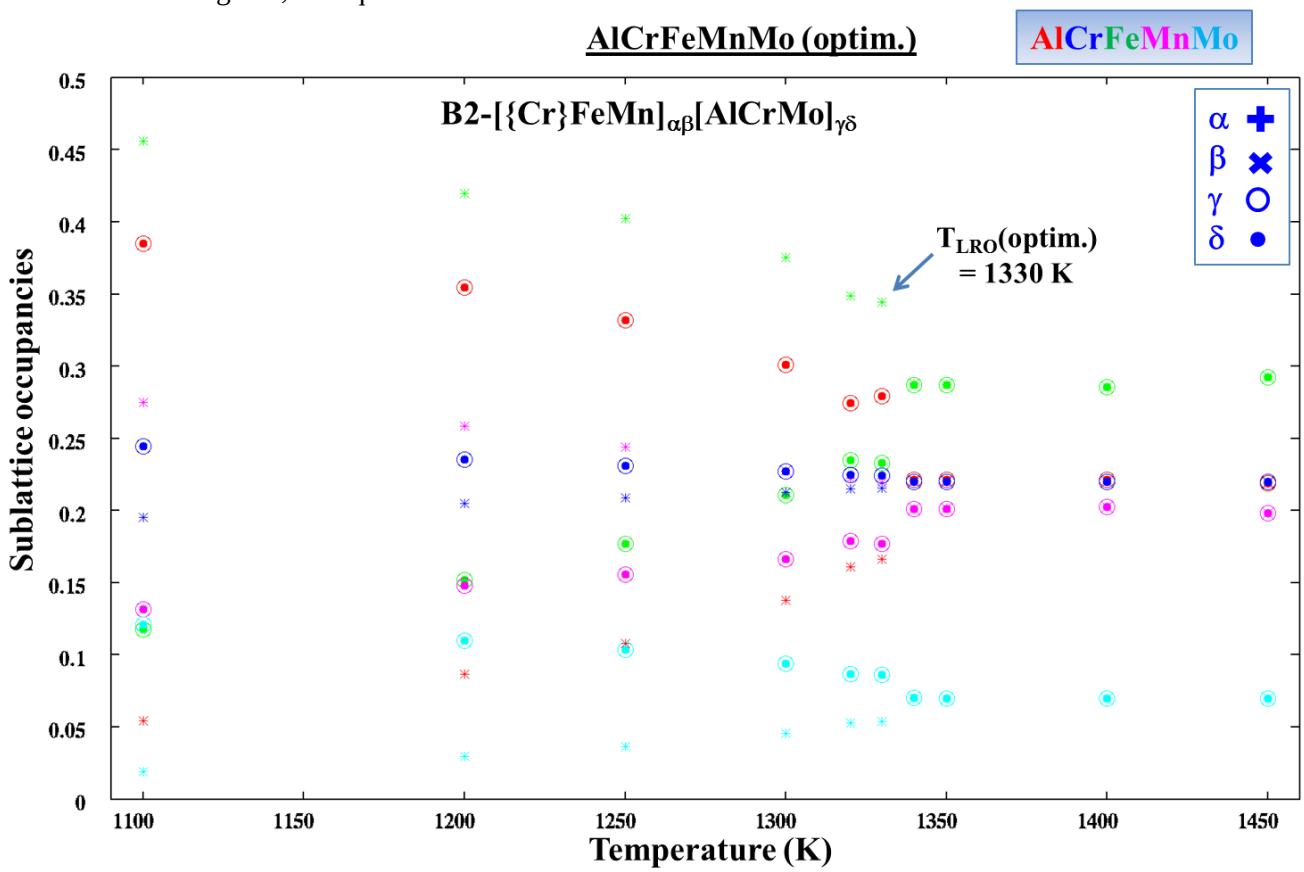

Figure A4: Same as Fig. A3, for "optimized" AlCrFeMnMo, with composition Al22Cr22Fe29Mn20Mo7 heuristically selected.